American Journal of Geosciences

Original Research Paper

Petrophysical Characterization and Flow Models for Agbada Reservoirs, Onshore Niger Delta, Nigeria

Prince Suka Momta, John Owate Etu-Efeotor and Charles Ugwu Ugwueze

Department of Geology, University of Port Harcourt, Nigeria

Article history
Received: 22-01-2015
Revised: 24-08-2015
Accepted: 16-09-2015

Corresponding Author:
Prince Suka Momta
Department of Geology,
University of Port Harcourt,
Nigeria
Email: princemomta@yahoo.com

Abstract: Three selected reservoirs (XB, XC and XE) from three wells (A, B and C) occurring within the Agbada producing sands in part of the Greater Ughelli Depobelt of the onshore Niger Delta have been studied. The study aims at evaluating the petrophysical characteristics of the sand-bodies and also identifies the various flow units present within each reservoir. Petrophysical parameters were used as input data to generate the Stratigraphic Modified Lorenzo Plots (SMLP). This model uses a graphical method to quantitatively determine flow units and to understand the flow and storage capacities of sedimentary rocks. Results of the analysis shows that average porosity and permeability range is between 7-28.8% and 1.20-529 mD, indicating poor to very good reservoir quality in different parts of the field. Generally, porosity and permeability decrease with increasing depth in the field reflecting burial diagenetic porosity loss in response to increasing thermal exposure with depth. Porosity and permeability change laterally across the field from west to east. Increase in porosity and permeability towards the eastern part of the field reflects lateral change in facies. Well C has the best porosity (28%) and permeability (529 mD), lowest water saturation (0.01), hence, highest hydrocarbon prospect. The stratigraphic Modified Lorenzo Plots (SMLP) revealed a total of seventy five (75) Flow Units (FU) in the three studied reservoirs. Each reservoir displays similar flow pattern relative to others suggesting that facies (rock properties) have a strong control on flow in each reservoir. Generally, poor quality units occur towards the bottom of each reservoir in a well and good quality units towards the top. The dominant flow units in the three reservoirs fall within the high storage and flow (normal flow unit) unit category, suggesting that the dominant depositional setting (shallow marine shoreface/beach/barrier) and facies type beside diagenetic effects play significant role in fluid dynamic behaviour of any rock body. Depositional environments and subsequent diagenesis are the primary factors controlling porosity distribution, pore connectivity and fluid flow in the three studied reservoirs.

Keywords: Shoreface Sand, Shallow Marine, Porosity, Permeability, Lorenzo Plot

Introduction

The study area falls within the onshore portion of the Niger Delta sedimentary basin in the Greater Ughelli depobelt. The Agbada stratigraphic unit forms the hub of oil and gas accumulation in the basin. Extensive studies have been carried out that gave insight into the gross depositional setting of the foreset beds of the Agbada reservoirs (Amajor and Agbaire, 1989; Reijers, 2011; Arochukwu, 2014). In the past one decade there had been slow exploration activities in the basin. Efforts have been concentrated on developing and producing from proven reserves in the various oilfields. This provided more job opportunities for reservoir engineers, production engineers, development geologists and petrophysicists than exploration geoscientists. Modern geostatistical computer software has also improved the understanding of reservoir conditions through modeling and simulation. Petrophysical parameters serve as input data that help in building these models that have given much insight into reservoir condition and improved oil and gas production.

The concept of hydraulic flow unit and petrophysics have been well documented in recent time (Amaefule *et al*., 1993; Abbaszadeh *et al*., 1996; Gunter *et al*., 1997a; 1997b; Porras *et al*., 1999; Al-Ajmi and Holditch, 2000; Yasin *et al*., 2001; Rushing and Newsham, 2001b; Aguilera and Aguilera, 2002; Civan, 2003; Tiab and Donaldson, 2004; Perez *et al*., 2005; Taslimi *et al*., 2008; Bhattacharya *et al*., 2008; Rahimpour-Bonab *et al*., 2012). In this study, the Stratigraphic Modified Lorenzo Plots by Gunter *et al*., (1997a) and adopted by Rahimpour-Bonab *et al*. (2014), will be adopted to identify flow units and also to understand the hydraulic behaviour of sand-bodies deposited within a specific depositional environment. Fractional flow capacity and storage capacity values are determined from inflection points on the Lorenzo plot, which correspond to changes in flow capacity or storage capacity associated with factors that affect reservoir quality. These changes are interpreted as flow units within the reservoir (Gunter *et al*., 1997a; Lawal and Onyekonwu, 2005; Rahimpour-Bonab *et al*., 2014). The Gunter *et al.* (1997a) model used a graphical method to quantitatively determine flow units. Petrophysical data will be used to accomplish these plots to understand the flow and storage capacities of sedimentary rocks.

Petrophysical parameters that will be generated from wireline logs (comprising of Gamma Ray, Resistivity, Neutron, Density and Sonic) include; true formation resistivity (R_t), formation water resistivity (R_w), formation factor (F), water saturation (S_w), irreducible water saturation (S_{wirr}), Bulk Volume Water (BVW), porosity and permeability. Deductions from the analysis and interpretation of petrophysical parameters will be useful in oil and gas production and reservoir management.

Geological Setting

The evolution of the Niger Delta sedimentary basin is controlled by pre- and synsedimentary tectonics as described by (Evamy *et al*., 1978; Ejedawe, 1981; Knox and Omatsola, 1989; Stacher, 1995; Reijers, 2011). The embryonic delta that developed following the subsidence that occurred down dip of the Upper Cretaceous Anambra basin during the Eocene time has continued to grow seaward from one time to the other. The growth and further development of the delta have been accentuated by high sediment supply, climatic factors and proximity of provenance areas. Initial sediment deposition during the Middle-Late Eocene time was towards the west of the inverted Cretaceous Abakaliki High and south of the Anambra Basin (Reijers, 2011). Studies by (Weber and Daukuro, 1975; Ejedawe, 1981; Ejedawe *et al*., 1984; Reijers, 2011), showed that the embryonic delta subsided during the Late Eocene to Middle Oligocene <700 m/Ma and prograded approximately 2 km/Ma along three depositional axes that fed irregular, early delta lobes that eventually coalesced. Recent study by Durogbitan (2014) has corroborated the fact that during the Miocene the delta was at the lowstand and experienced high fluvial incision that led to the formation of most of the channels (Opuama). He argued that the delta at that time was actually fluvial-dominated which does not actually portray the picture of the present day wave-dominated delta. Adojoh *et al*. (2014), demonstrated from palynology point of view that hinterland pollen and very fine sand and siltstones have been deposited during dry climatic periods. Momta and Odigi (2014), described the Lowstand Systems Tracts (LST) associated with shallow marine Tortonian section of the Eastern Niger Delta, as being fluvially-induced rather than a deep sea turbidite LST. The progradation of the Niger Delta has continued from the Eocene to the present day with an advancing coastline.

Three diachronous stratigraphic units have been identified in the subsurface of the Niger Delta. The basal unit is the Akata shale of Eocene age, which is believed to be the stratigraphic equivalence of the exposed Paleocene Imo shales north of the Niger Delta, Reijers (2011) and the major source rock. The Agbada Group, Reijers (2011), which is a sequence of shale and sand in almost equal proportions overlies the Akata group, Reijers (2011) and constitutes majorly the hydrocarbon producing portion of the delta. The youngest Benin Group is the topset portion of the delta made of majorly very coarse grained loose sands with gravels, peat/wood materials and minor clay intervals. Eleven megasequences have been identified beginning from the Northern Delta Depobelt to the Coastal Swamp Depobelt based on the presence of regionally continuous transgressive shales that contain distinct biostratigraphic records. The youngest of this shale is the Bolivina 46 shale (Qua Iboe Shale) which also continued up to the shallow offshore area in the eastern part of the Niger Delta.

Materials and Methods

This study examined three selected reservoirs (XB, XC and XE) from three wells designated A, B and C. A suite of well logs consisting of Gamma Ray (GR), resistivity (ILD), Neutron, Density and Sonic were provided for this study. Petrophysical parameters were deduced from log data and used to characterize the reservoirs. Poroperm calculations were basically based on the Archie's petrophysical equations (Archie, 1950). Gamma ray log gives information on the lithology types encountered in the field. Petrophysical parameters were first generated for the three selected reservoirs using well logs. The Gunter *et al*. (1997a), method was adopted to subdivide the reservoirs into Flow units. Flow unit demarcation is useful in reservoir modeling and flow simulation (Amaefule *et al*., 1993; Bhattacharya *et al.*, 2008; Rahimpour-Bonab *et al*., 2012; 2014). Gunter *et al.*

(1997a; 1997b) presented a graphical method for quantifying the flow units according to the petrophysical rock/pore types, flow and storage capacities (Kh) and (Φh) and reservoir process speed (K/Φ). In this study, the minimum numbers of static flow units have been determined using the static reservoir rock properties such as log poroperm values. A Stratigraphic Modified Lorenz Plot (SMLP) was generated using cumulative flow capacity (Khcum) and cumulative storage capacity (Φhcum). The flow capacity (Kh) and storage capacity (Φh) are functions of permeability and porosity values considering their sampling depths (Equation 1 and 2). The values of cumulative flow and storage capacities were determined using Equation 3 and 4 (Rahimpour-Bonab *et al*., 2014; Gunter *et al*., 1997a):

$$Kh = K1(h1 - h0), K2(h2 - h1),..., Kn(hn - hn - 1) \quad (1)$$

$$\Phi h = \Phi 1(h1 - h0), \Phi 2(h2 - h1),...., \Phi n(hn - hn - 1) \quad (2)$$

$$Khcum = K1(h1 - h0) / KhTotal + K2(h2 - h1) /KhTotal + ... + Kn .....(hn - hn - 1) / KhTotal \quad (3)$$

$$\Phi hcum = \Phi 1(h1 - h0) / \Phi hTotal + \Phi 2(h2 - h1) /\Phi hTotal + ... + \Phi n(hn - hn - 1) / \Phi hTotal \quad (4)$$

Where:
K = Permeability (mD)
h = Sample depth (m)
Φ = Fractional porosity

The various points of inflection show the number of flow units in the Stratigraphic Modified Lorenzo Plot (SMLP).

Study Location

The study area is an onshore Niger Delta field, located in the Greater Ughelli Depobelt (Fig. 1). Three wells (A,B and C) (Fig. 1) studied in the area are separated at a distance of about 8 km between A and B, B and C and about 15.2 km between A and C covering an area of approximately 18.9 Sq.km (Fig. 1). The wells are separated by a set of minor faults and two major faults (red curved lines in Fig. 1) that appear to be regional as represented on the base map. These faults followed the growth faulting pattern of the Niger Delta as observed on seismic section.

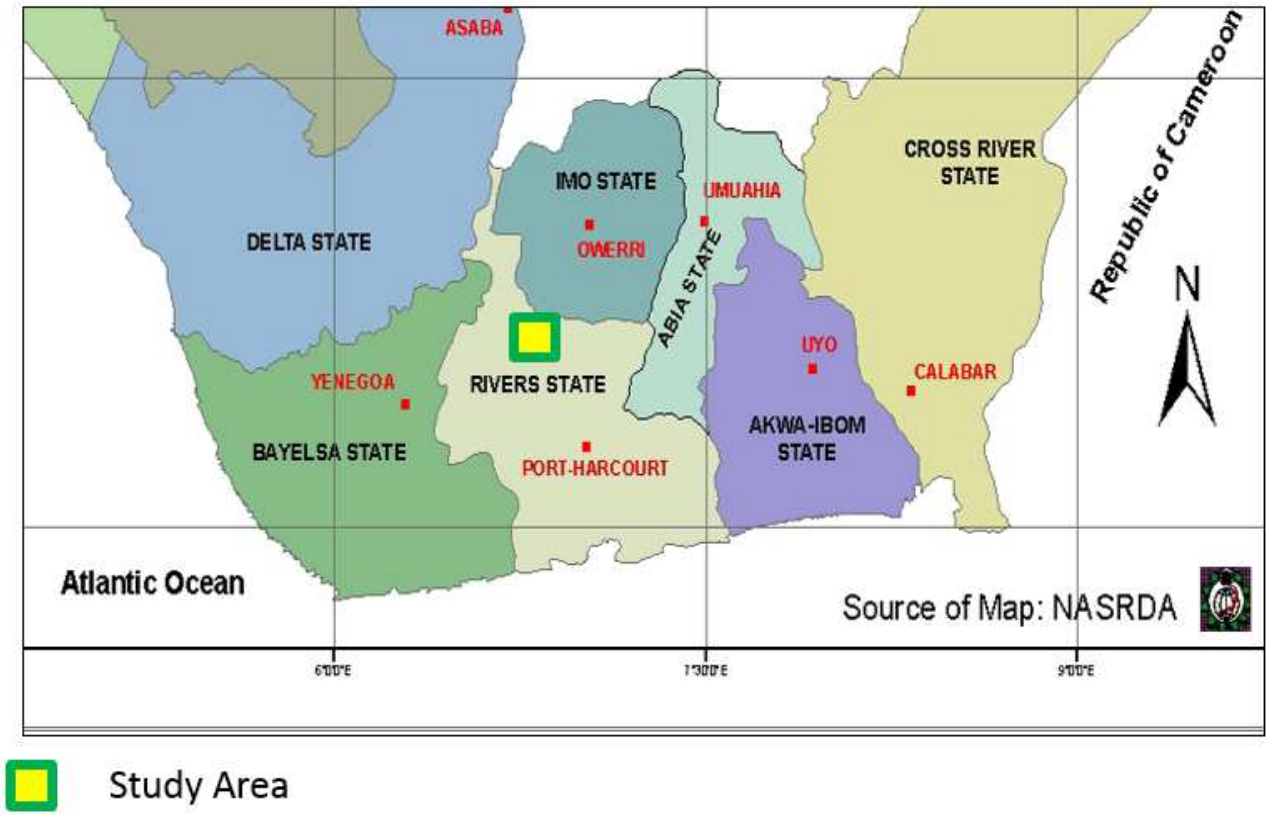

Fig. 1. Map showing study area and well locations

The main body of the study area is dissected by several minor to intermediate faults which do not presently appear to impede fluid communication within the major reservoirs.

Results

Reservoir Quality Assessment

Petrophysical evaluation of three reservoirs (XB, XC and XE) carried out shows average porosity and permeability range to be between 7-28.8% and permeability 1.20-529 mD (Table 1). This implies that the reservoir property ranges from poor to very good at different parts of the field. Generally, porosity and permeability decrease with increasing depth in the field. This trend reflects burial diagenetic porosity loss in response to increasing thermal exposure with depth (Ehrenberg and Nadeau, 2005). It is also observed that porosity and permeability change laterally across the field from west to east. Wells A and B have the poorest porosity and permeability. They occur towards the western part of the field. This increase in porosity and permeability towards the eastern part of the field reflects lateral change in facies. Well A occurred towards the basin-ward side of the field and may indicate that there is a shift from lower marine mud/silt dominated environment to the shoreface/coastal environment where porosity is high. Well C has the best porosity and permeability, lowest water saturation, hence, highest hydrocarbon prospect. The density-neutron crossover is also detected in well C showing the presence of a gas cap. This occurs at depth 3350 m (Table 1).

Reservoir Description

Reservoir XB

This reservoir has a funnel shaped GR log motif indicating an upward coarsening sequence of increasing grain size (Fig. 2). It occurs at a depth of about 2835 m in well A, 2760 m in B and 2680 m in well C. It has a range of porosity between 7-13% and average porosity of 9.37% (Table 1) in well A. Its permeability is between 0.4 to 3.6 mD and average permeability of 1.2 mD. Water saturation is very high, average of 88%. This reservoir has low hydrocarbon potential with its high water saturation content. In well C, there is an increase in porosity and permeability. Neutron-Density corrected porosity range is between 15-46% and average porosity is 28.8%. Permeability range is between 55-1673 mD with average value of 529 mD. Average water saturation is 1.9%. Reservoir XB in well C shows great hydrocarbon prospect with its good to very good petrophysical characteristics.

Reservoir XC

This also displays a funnel shaped GR motif. It shows a prograding stacking pattern of a sand body increasing in grain size upward. This unit is similar to XB and XE. The top of reservoir XC occurred at 3040, 2925 and 2825 m in wells A, B and C, with average thickness of 122 m. Its range of porosity and permeability in well A is between 5.6-9.2% and 0.3-0.8 mD. Average porosity and permeability is 7.8% and 0.5 mD. It has high water saturation in well A and less hydrocarbon potential. No geophysical measurement was done for this reservoir in well B. In well C, its average porosity and permeability are 24.4% and 270.7 mD. Water saturation is very low (1.1%). The depositional setting of this sand-body might be mouth bars, interdistributary beach and deltaic front facies (upper shoreface).

Reservoir XE

This reservoir also displays a coarsening upward trend. It occurs in all the wells with thicknesses of 55, 65 and 95 m in wells A, B and C. Top of this reservoir occurs at 3610, 3455 and 3245 m. The GR log motif displays a serrated funnel shape trend indicating progradation with within impacts of tidal activities. It represents deposit within the delta front environment. Porosity and permeability values in well A show an average of 11.5% and 0.57 mD. Water saturation is 86%. In well B, porosity and permeability range is between 0.7-10.3% and 0.2-8.8 mD. Average water saturation is 50% (Table 1). In well C, porosity and permeability is good with an average of 11.6% and 56.6 mD. Water saturation is very low, 0.9%. This reservoir has a tendency of producing more water than hydrocarbon in well A and B and more hydrocarbon than water in well C.

Sedimentology and Depositional Environments

The Gamma Ray log trends have been used to infer both lithology types and gross depositional environments of the three sand bodies. The general trend for the reservoirs shows a coarsening upward gamma ray log motif, indicating an increase in grain size (Fig. 2). Environments that display this attribute range from beach, barrier to upper shoreface deposits. Gamma Ray (GR) with 100°API and above contains majorly a clay/mud or shale-dominated environments. Gamma ray values below 75°API tend towards sand. Quantitatively, GR log have been used to compute values for gamma ray index and consequently for volume of shale (Vsh).

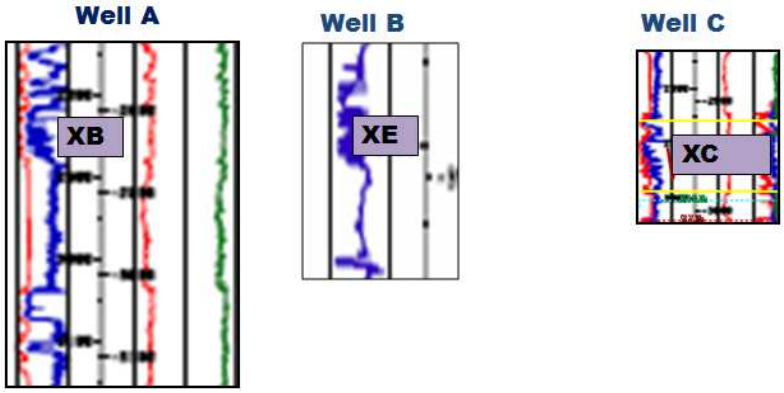

Fig. 2. Wells A, B and C showing the Coarsening Upward (CU) sequences of reservoirs XB, XC and XE

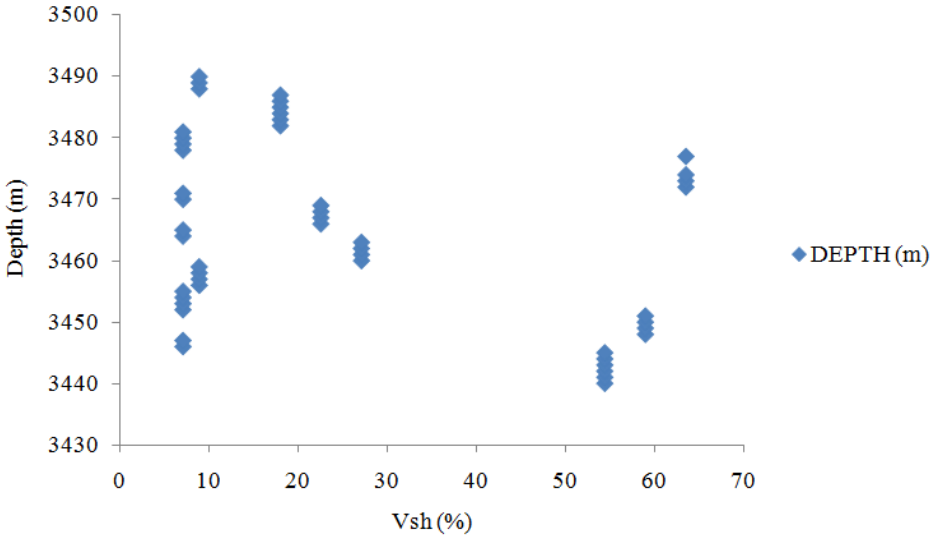

Fig. 3. Plot of volume of shale against depth for reservoir Xe in well

Table 1. Petrophysical summary for reservoirs Xb, Xc and Xe

Depth (m)	Well	Reservoir	Φ	S_w	S_h	K (mD)
3180-3244	A	XB	9.4	0.88	0.12	1.2
3592-3640	A	XC	7.41	0.86	0.14	0.57
3740-3780	A	XE	11.5	0.85	0.15	45
2672-2700	B	XB	-	-	-	-
3440-3490	B	XC	-	-	-	-
3584-3700	B	XE	5.5	0.55	0.45	2.72
3016-3064	C	XB	28.81	0.02	0.98	529
2856-2992	C	XC	24.38	0.01	0.99	270
32482-3340	C	XE	11.6	0.01	0.99	56.6

Volume of Shale (Vsh)

The plot for volume of shale shows a high percentage of shale towards the lower part of Reservoir XE in well B (Fig. 3). The observed depositional setting is the main controlling factor for Vsh distribution in this reservoir. The selected reservoirs have similar trend and may represent similar depositional setting, probably upper shoreface or regressive bars (barrier bars). The lower portion of the reservoir may represent a lower shoreface/shoreface transition environment dominated by mud/silty and very fine grained sandstones. The three reservoirs may likely exhibit similar flow behaviour due to their similarities in electrofacies trend (Fig. 2) and flow plots, though may vary in saturation types and amount. Higher flow will be experienced towards the top of the reservoirs.

DOI: 10.3844/ajgsp.2015.40.52

Flow Unit Determination

A total of seventy five (75) flow units have been identified from the SMLP for the three reservoirs. The major controlling factors accounting for the hydraulic delimitation of each sand body are the facies characteristics and petrophysical parameters evolving from the relationship in rock fabrics. The break or inflection points revealed the number of preliminary flow units in the Stratigraphic Modified Lorenzo Plots. In this study, three main types of flow units have been defined based on Rahimpour-Bonab's model: Normal flow units: With approximately high or equal values of the storage and flow capacities (FU3, FU6 and FU8 in Fig. 4-10); baffle units, with low flow capacity and high storage capacity; and finally, barrier units, containing impermeable units with very low flow and storage capacities. The slope of each segment is indicative of the flow performance in the reservoir (Gunter *et al.*, 1997a). Steep slopes are indicative of permeable and high performance flow units (Rahimpour-Bonab *et al*., 2014) and gentle slopes or horizontal segments are representative of low permeability units or flow barriers.

The normal flow units as mentioned above have approximately equal flow and storage capacities. They are recognized with it straight or high angle gradient (about 15 or 345° from the normal) on the SMLP. This unit occurs in all the reservoirs and in all the wells (Fig. 4a-10). There are about thirty-eight (38) units that exhibit this flow and storage capacities. In well A, reservoir XB, they occur in FU1, FU2, FU3, FU4, FU7, FU8 and FU9; in reservoir XC, they occur in FU1, FU3, FU4, FU11; in reservoir XE as FU2, FU3, FU4, FU6, FU8 and FU9 (Fig. 4a-10).

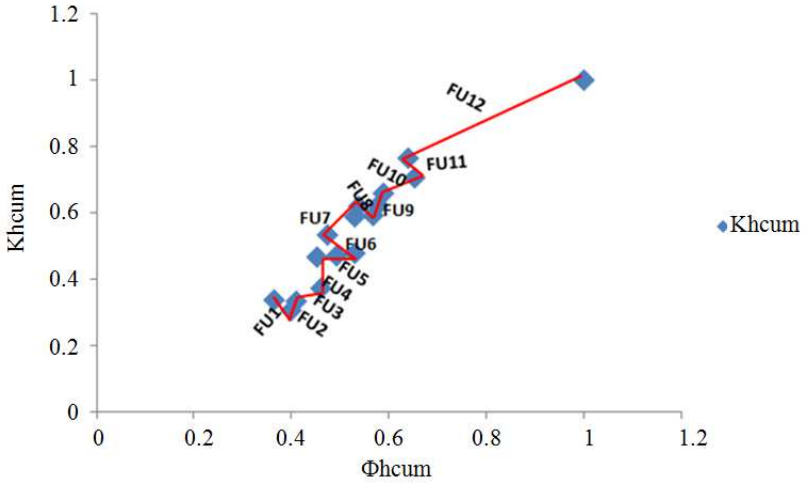

Fig. 4. Stratigraphic Modified Lorenzo Plot (SMLP) of cumulative flow capacity (Khcum) versus cumulative storage capacity (Φhcum) for well A, reservoir XB. FU = Flow Unit

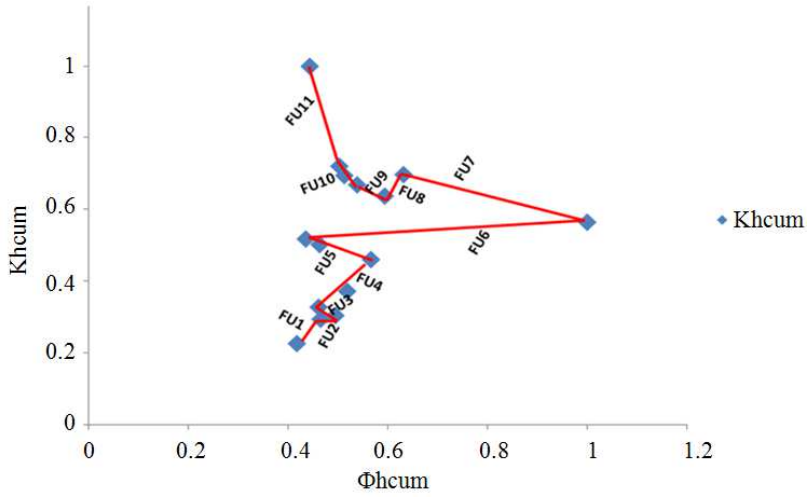

Fig. 5. SML plot of cumulative flow capacity (Khcum) versus cumulative storage capacity (Φhcum) for well A, reservoir XC

DOI: 10.3844/ajgsp.2015.40.52

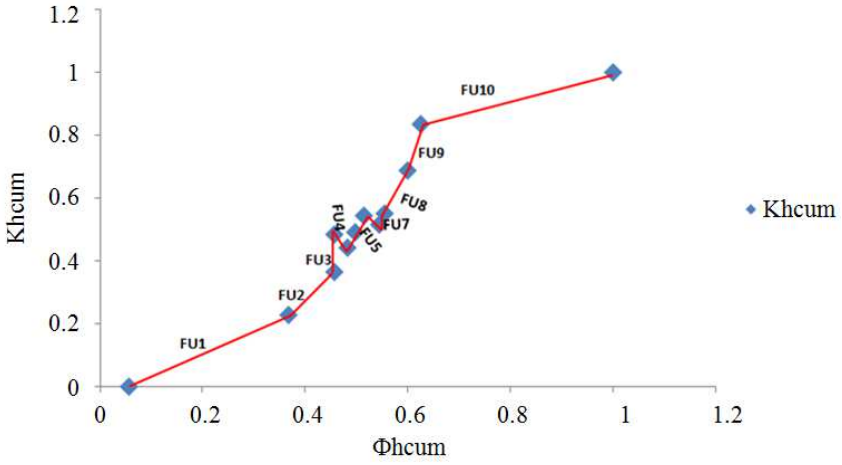

Fig. 6. SML plot of cumulative flow capacity (Khcum) versus cumulative storage capacity (Φhcum) for well A, reservoir XE. FU = Flow Unit

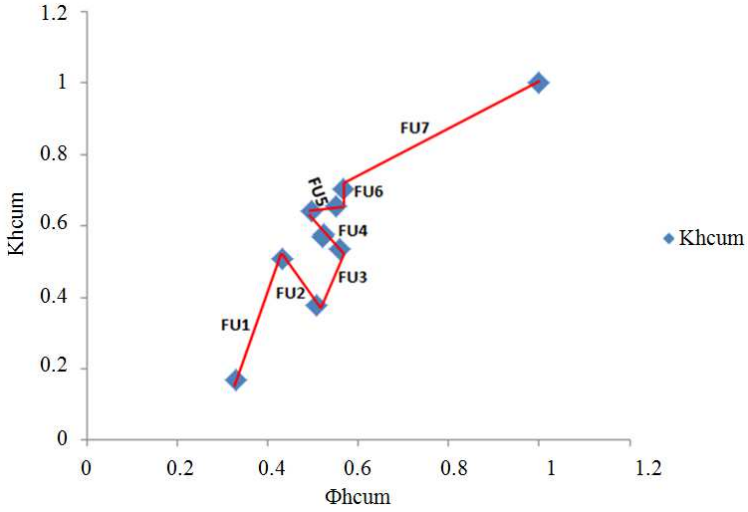

Fig. 7. SML plot of cumulative flow capacity (Khcum) versus cumulative storage capacity (Φhcum) for well B, reservoir XB

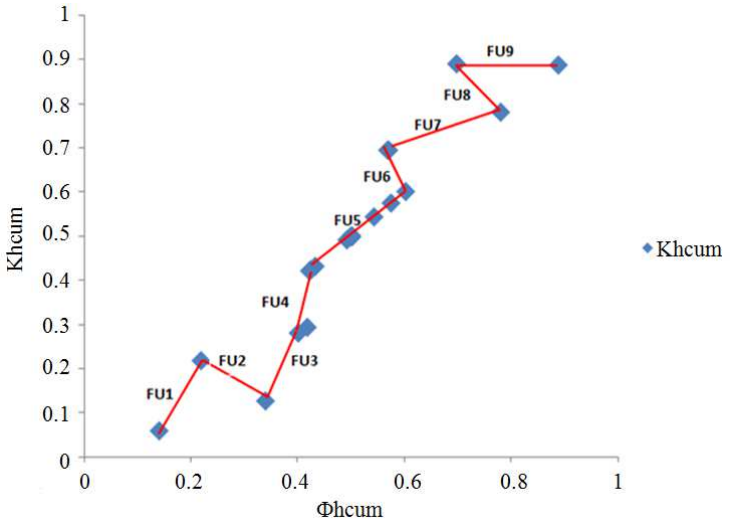

Fig. 8. SML plot of cumulative flow capacity (Khcum) versus cumulative storage capacity (Φhcum) for well B, reservoir XE

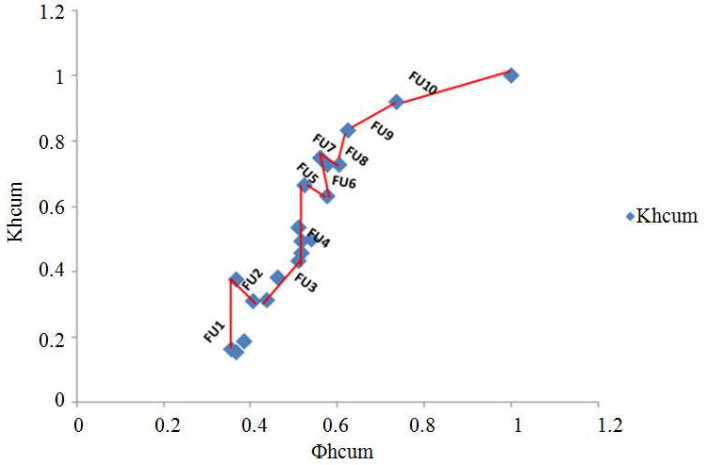

Fig. 9. SML plot of cumulative flow capacity (Khcum) versus cumulative storage capacity (Φhcum) for well C, reservoir XC

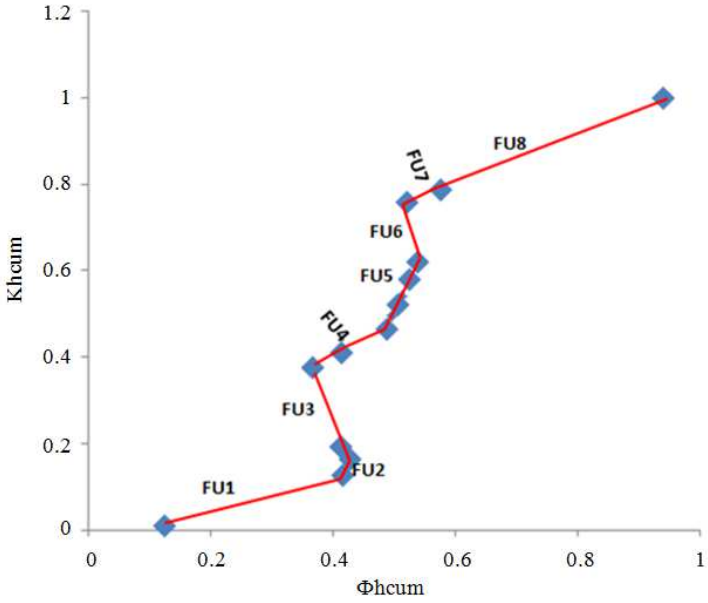

Fig. 10. SML plot of cumulative flow capacity (Khcum) versus cumulative storage capacity (Φhcum) for well C, reservoir XE

Discussion

In well B (XB and XE include: FU1, FU2 FU4 and FU1 FU3, FU4, FU5, FU6, FU8) and finally, in well C, they include FU1, FU3, FU4, FU5, FU6, FU8, FU9 (Reservoir XC) and FU2, FU3, FU4, FU5, FU6 (reservoir XE), Fig. 4-10. It is obvious that the units with the highest flow and storage capacities dominate in all the reservoirs. This shows that sediments deposited within shallow marine beach, barrier and shoreface environments as indicated by the log motif (Fig. 3) have good reservoir qualities. The general trend of the speed velocity, a ratio of permeability and porosity (Table 2-7), increases towards the top of the reservoirs. The speed velocity gives information about the pore throat characteristics. This implies that megaporous units are developed towards the top of the reservoirs.

The baffle units have low flow and high storage capacities (FU10, FU12 (well A reservoir XB), FU5, FU7 (A, XC), FU1 (XE); well B contains FU5, FU7 (in XB), FU7 (in XE); well C has FU10 in XC and FU1 and FU8 in reservoir XE (Fig. 4-10). The baffle units are: FU5, FU6; FU2, FU6, FU8, FU9, FU10 in reservoirs XC and XE for well A. Well B has FU3, FU6; FU2, FU9 (for reservoirs XB and XE); FU2, FU7; FU7 for well C, reservoirs XC and XE (Fig. 4-10). This unit shows areas with very low porosities and permeabilities. This may have been caused by the presence of shale that occurred as intercalations in the reservoirs and also the lower part of the reservoirs stratigraphically fall within the lower shoreface dominated by silty/mud or shaly facies. The slope of this unit on the SMLP is very low (horizontal or almost horizontal).

DOI: 10.3844/ajgsp.2015.40.52

Table 2. Well a, reservoir Xb (Stratigraphic Modified Lorenzo Plot Parameters)

Depth (m)	Thickness (h)	Φ	K (MD)	Process SpeedK/Φ	Φh	ΦhTotal	Kh	KhTotal	Φhcum	Khcum
2816	3	8.874360	0.938127	0.1057121	26.62308	26.62308	2.814381	2.814381	1.000000	1.000000
2819	3	8.577360	0.842740	0.0982517	25.73208	52.35516	2.528220	5.342601	0.491491	0.473219
2824	5	9.652500	1.222490	0.1266501	48.26250	73.99458	6.112450	8.640670	0.652244	0.707405
2829	5	8.206110	0.733099	0.0893358	41.03055	89.29305	3.665495	9.777945	0.459504	0.374874
2833	4	7.092360	0.463042	0.0652874	28.36944	69.39999	1.852168	5.517663	0.408782	0.335680
2838	5	8.167500	0.722288	0.0884344	40.83750	69.20694	3.611440	5.463608	0.590078	0.660999
2842	4	9.171360	1.040629	0.1134651	36.68544	77.52294	4.162516	7.773956	0.473220	0.535444
2847	5	9.616860	1.208328	0.1256468	48.08430	84.76974	6.041640	10.20416	0.567234	0.592076
2851	4	9.913860	1.329825	0.1341380	39.65544	87.73974	5.319300	11.36094	0.451967	0.468209
2856	5	8.984250	0.975209	0.1085465	44.92125	84.57669	4.876045	10.19535	0.531130	0.478262
2861	5	10.50786	1.597349	0.1520147	52.53930	97.46055	7.986745	12.86279	0.539083	0.620919
2865	4	8.725860	0.889561	0.1019454	34.90344	87.44274	3.558244	11.54499	0.399158	0.308207
2870	5	9.542610	1.179184	0.1235704	47.71305	82.61649	5.895920	9.454164	0.577525	0.623632
2873	3	9.097110	1.014322	0.1114994	27.29133	75.00438	3.042966	8.938886	0.363863	0.340419
2876	3	10.21086	1.459406	0.1429268	30.63258	57.92391	4.378218	7.421184	0.528842	0.589962
2880	4	13.60212	3.601564	0.2647796	54.40848	85.04106	14.40626	18.78447	0.639791	0.766924

Table 3. Petrophysical parameters for well a, reservoir Xc

Depth (m)	Thickness (h)	Porosity (Φ)	K (mD)	Proc. Speed) (K/Φ)	Φh	ΦhTotal	Kh	KhTotal	Φhcum	KhcumQ
3044	4	7.612110	0.578590	0.0760091	30.44844	30.44844	2.314360	4.10255	1.0000000	0.5641272
3049	5	6.534000	0.357638	0.0547349	32.67000	63.11844	1.788190	4.804978	0.5175983	0.3721536
3053	4	8.280360	0.754197	0.0910826	33.12144	65.79144	3.016788	4.190983	0.5034308	0.7198283
3058	5	5.717250	0.234839	0.0410755	28.58625	61.70769	1.174195	2.342471	0.4632526	0.5012634
3062	4	6.127110	0.292069	0.0476683	24.50844	53.09469	1.168276	3.560701	0.4615987	0.3281028
3067	5	7.166610	0.478485	0.0667659	35.83305	60.34149	2.392425	3.748553	0.5938377	0.6382263
3071	4	6.424110	0.339032	0.0527749	25.69644	61.52949	1.356128	5.982778	0.4176280	0.2266720
3076	5	8.835750	0.925330	0.1047257	44.17875	69.87519	4.626650	6.649990	0.6322523	0.6957379
3081	5	6.795360	0.404668	0.0595506	33.97680	78.15555	2.023340	3.910645	0.4347330	0.5173929
3086	5	6.646860	0.377461	0.0567879	33.23430	67.21110	1.887305	6.217540	0.4944764	0.3035453
3091	5	8.651966	0.866047	0.1000983	43.25983	76.49413	4.330235	9.401845	0.5655314	0.4605729
3096	5	9.09711	1.014322	0.1114994	45.48555	88.74538	5.07161	7.295192	0.5125399	0.6951990
3102	6	6.60825	0.370597	0.0560810	39.64950	85.13505	2.223582	7.560577	0.4657248	0.2941022
3107	5	9.24561	1.067399	0.1154493	46.22805	85.87755	5.336995	7.971575	0.5383019	0.6695032
3112	5	7.38936	0.526916	0.0713074	36.94680	83.17485	2.63458	2.63458	0.4442064	1.0000000

Table 4a. Petrophysical parameters for well a, Reservoir Xe

Depth (m)	Thickness (h)	Porosity (Φ)	K (MD)	Proc. Speed (K/Φ)	Φh	ΦhTotal	Kh	KhTotal	Φhcum	Khcum
3612	8	65.13441	500.1877	7.6793157	521.0753	521.0753	4001.502	4001.502	1.000000	1.000000
3620	4	7.686360	0.596554	0.0776120	30.74544	551.8207	2.386216	4003.888	0.055716	0.000596
3624	4	7.128000	0.470412	0.0659949	28.51200	59.25744	1.881648	4.267864	0.481155	0.440888
3628	4	7.053750	0.455148	0.0645257	28.21500	56.72700	1.820592	3.702240	0.497382	0.491754
3632	4	7.464412	0.543959	0.0728737	29.85765	58.07265	2.175836	3.996428	0.514143	0.544445
3636	5	7.092271	0.463024	0.0652857	35.46136	65.31900	2.315120	4.490956	0.542895	0.515507
3641	4	5.162008	0.170219	0.0329753	20.64803	56.10939	0.680876	2.995996	0.367996	0.227262
3645	5	5.123250	0.166226	0.0324454	25.61625	46.26428	0.831130	1.512006	0.553694	0.549687
3650	4	5.384610	0.194431	0.0361087	21.53844	47.15469	0.777724	1.608854	0.456761	0.483402
3654	5	6.459750	0.344992	0.0534064	32.29875	53.83719	1.724960	2.502684	0.599934	0.689244
3659	5	5.420250	0.198514	0.0366245	27.10125	59.40000	0.992570	2.717530	0.456250	0.365247
3664	5	9.058500	1.000823	0.1104844	45.29250	72.39375	5.004115	5.996685	0.625641	0.834480

Table 4b. Well B, Reservoir Xb

Depth (m)	Thickness (h)	Φ	K	Proc. Speed	Φh	ΦhTotal	Kh	KhTotal	Φhcum	Khcum
2672	2	31.82	523.640	16.45631678	63.640	63.640	523.640	523.640	1.000000000	1.000000000
2676	4	24.77	238.030	9.609608397	99.080	162.72	952.120	1475.76	0.608898722	0.645172657
2679	3	16.35	64.2400	3.929051988	49.050	148.13	192.720	1144.84	0.331128063	0.168337934
2683	4	15.61	55.5600	3.559256887	62.440	111.49	222.240	414.960	0.560050229	0.535569693
2686	3	20.59	132.900	6.454589607	61.770	124.21	398.700	620.940	0.497302955	0.642091023
2689	3	27.07	314.690	11.62504618	81.210	142.98	944.070	1342.77	0.567981536	0.703076476
2692	3	29.60	417.170	14.09358108	88.800	170.01	1251.51	2195.58	0.522322216	0.570013391
2695	3	36.24	789.200	21.77704194	108.72	197.52	2367.60	3619.11	0.550425273	0.654193987
2698	3	40.07	1082.50	27.01522336	120.21	228.93	3247.50	5615.10	0.525095007	0.578351232
2700	2	46.01	1673.24	36.36687677	92.020	212.23	3346.48	6593.98	0.433586204	0.507505331

Table 5. Well B Reservoir Xe

Depth (m)	Thickness (h)	Φ_{dcorr}	K(MD)	Process SpeedK/Φ	Φh	ΦhTotal	Kh	KhTotal	Φhcum	Khcum
3440	1	3.295097	1.821576	0.5528141	3.295097	3.2950970	1.821576	1.821576	1.0000000	1.0000000
3441	1	3.295097	1.821576	0.5528141	3.295097	6.5901940	1.821576	3.643152	0.5000000	0.5000000
3442	1	3.295097	1.821576	0.5528141	3.295097	6.5901940	1.821576	3.643152	0.5000000	0.5000000
3443	1	3.295097	1.821576	0.5528141	3.295097	6.5901940	1.821576	3.643152	0.5000000	0.5000000
3448	5	4.836095	4.122913	0.8525294	4.836095	15.163075	4.122913	12.926966	0.3189389	0.3189390
3449	1	4.836095	4.122913	0.8525294	4.836095	9.6721900	4.122913	8.2458260	0.5000000	0.5000000
3450	1	0.790787	0.253972	0.3211636	0.790787	5.6268820	0.253972	4.3768850	0.1405373	0.0580257
3451	1	0.790787	0.253972	0.3211636	0.790787	1.5815740	0.253972	0.5079440	0.5000000	0.5000000
3452	1	6.281671	2.017445	0.3211637	6.281671	7.0724580	2.017445	2.2714170	0.8881878	0.8881879
3453	1	6.281671	2.017445	0.3211637	6.281671	12.563342	2.017445	4.0348900	0.5000000	0.5000000
3454	1	6.281671	2.017445	0.3211637	6.281671	12.563342	2.017445	4.0348900	0.5000000	0.5000000
3455	1	6.281671	2.017445	0.3211637	6.281671	12.563342	2.017445	4.0348900	0.5000000	0.5000000
3456	1	6.089008	1.955569	0.3211638	6.089008	12.370679	1.955569	3.9730140	0.4922129	0.4922130
3457	1	6.089008	1.955569	0.3211638	6.089008	12.178016	1.955569	3.9111380	0.5000000	0.5000000
3458	1	8.111662	4.484239	0.5528138	8.111662	14.200670	4.484239	6.4398080	0.5712169	0.6963312
3459	1	8.111662	4.484239	0.5528138	8.111662	16.223324	4.484239	8.9684780	0.5000000	0.5000000
3460	1	6.185036	3.419174	0.5528139	6.185036	14.296698	3.419174	7.9034130	0.4326199	0.4326199
3461	1	6.185036	3.419174	0.5528139	6.185036	12.370072	3.419174	6.8383480	0.5000000	0.5000000
3462	1	4.162383	1.336807	0.3211639	4.162383	10.347419	1.336807	4.7559810	0.4022629	0.2810791
3463	1	4.162383	1.336807	0.3211639	4.162383	8.3247660	1.336807	2.6736140	0.5000000	0.5000000
3464	1	6.281671	2.017445	0.3211637	6.281671	10.444054	2.017445	3.3542520	0.6014591	0.6014590
3465	1	6.281671	2.017445	0.3211637	6.281671	12.563342	2.017445	4.0348900	0.5000000	0.5000000
3466	1	4.644039	1.491497	0.3211638	4.644039	10.925710	1.491497	3.5089420	0.4250560	0.4250560
3467	1	4.644039	1.491497	0.3211638	4.644039	9.2880780	1.491497	2.9829940	0.5000000	0.5000000
3468	1	4.644039	1.491497	0.3211638	4.644039	9.2880780	1.491497	2.9829940	0.5000000	0.5000000
3469	1	4.644039	1.491497	0.3211638	4.644039	9.2880780	1.491497	2.9829940	0.5000000	0.5000000
3470	1	6.281671	2.017445	0.3211637	6.281671	10.925710	2.017445	3.5089420	0.5749440	0.5749440
3471	1	8.304325	4.590746	0.5528139	8.304325	14.585996	4.590746	6.6081910	0.5693355	0.6947054
3474	1	2.331784	1.289043	0.5528141	2.331784	4.6635680	1.289043	2.5780860	0.5000000	0.5000000
3477	1	2.331784	1.289043	0.5528141	2.331784	4.6635680	1.289043	2.5780860	0.5000000	0.5000000
3478	1	8.304325	4.590746	0.5528139	8.304325	10.636109	4.590746	5.8797890	0.7807672	0.7807671
3489	11	6.089008	1.955569	0.3211638	6.089008	12.178016	1.955569	3.9111380	0.5000000	0.5000000
3490	1	6.089008	1.955569	0.3211638	6.089008	12.178016	1.955569	3.9111380	0.5000000	0.5000000

Table 6 Petrophysical Parameters for Well C, Reservoir XC

Depth (m)	Thickness (h)	ΦND corr	K (MD)	Process Speed K/Φ	Φh	ΦhTotal	Kh	KhTotal	Φhcum	Khcum
2856	7	25.77960	269.8670	10.46823845	180.4572	180.4570	1889.069	1889.07	1.000001	0.999999
2863	6	38.39097	946.1314	24.64463388	230.3458	410.8030	5676.788	7565.857	0.560721	0.750317
2869	5	31.56334	510.5712	16.17608276	157.8167	388.1625	2552.856	8229.644	0.406574	0.310202
2874	5	18.38339	93.01869	5.059931275	91.91695	249.7337	465.0935	3017.949	0.368060	0.154109
2879	5	14.31764	42.32774	2.956334983	71.58820	163.5052	211.6387	676.7322	0.437835	0.312736
2884	5	23.81233	210.1629	8.825801591	119.0617	190.6499	1050.815	1262.453	0.624504	0.832359
2889	6	21.24450	146.7088	6.905730895	127.4670	246.5287	880.2528	1931.067	0.517047	0.455837
2895	5	27.95040	348.1385	12.45558203	139.7520	267.2190	1740.693	2620.945	0.522987	0.664147
2900	5	23.97036	214.5877	8.952210146	119.8518	259.6038	1072.939	2813.631	0.461672	0.381336
2905	6	20.74186	136.0505	6.559223715	124.4512	244.3030	816.3030	1889.242	0.509413	0.432080
2911	6	21.70718	157.0112	7.233145899	130.2431	254.6942	942.0672	1758.370	0.511370	0.535762
2917	7	28.30714	362.3283	12.79989077	198.1500	328.3931	2536.298	3478.365	0.603393	0.729164
2924	7	17.74323	83.19217	4.688671116	124.2026	322.3526	582.3452	3118.643	0.385300	0.186730
2931	10	34.48271	674.6433	19.56468329	344.8271	469.0297	6746.433	7328.778	0.735192	0.920540
2941	9	21.24878	146.8020	6.908726054	191.2390	536.0661	1321.218	8067.651	0.356745	0.163767
2950	11	23.62307	204.9459	8.675667473	259.8538	451.0928	2254.405	3575.623	0.576054	0.630493
2961	14	21.85476	160.3984	7.339289015	305.9666	565.8204	2245.578	4499.983	0.540749	0.499019
2975	8	22.24566	169.6105	7.624431013	177.9653	483.9319	1356.884	3602.462	0.367749	0.376655
2983	9	21.23718	146.5498	6.900624283	191.1346	369.0999	1318.948	2675.832	0.517840	0.492911
2992	9	28.99696	390.8769	13.47992686	260.9726	452.1073	3517.892	4836.840	0.577236	0.727312

Table 7. Well C, Reservoir Xe

Depth (m)	Thickness (h)	ΦND Corr	K (MD)	Process SpeedK/Φ	Φh	ΦhTotal	Kh	KhTotal	Φhcum	Khcum
3248	6	33.30579	604.7376	18.1571312	199.83474	199.834700	3628.4256	3628.42600	1.0000002	0.99999989
3254	6	12.93482	30.73800	2.37637632	77.608920	277.443660	184.42800	3812.85360	0.27972858	0.04837007
3260	6	13.63049	36.25272	2.65967841	81.782940	159.391860	217.51632	401.944320	0.51309358	0.54116033
3266	6	13.99858	39.42708	2.81650567	83.991480	165.774420	236.56248	454.078800	0.50666128	0.52097231
3272	6	15.49649	54.30809	3.50454135	92.978940	176.970420	325.84854	562.411020	0.52539255	0.57937794
3278	6	14.81369	47.12150	3.18094276	88.882140	181.861080	282.72900	608.577540	0.48873646	0.46457350
3285	7	8.948296	9.629683	1.07614712	62.638072	151.520212	67.407781	350.136781	0.41339747	0.19251842
3290	5	8.871691	9.372383	1.05643704	44.358455	106.996527	46.861915	114.269696	0.41457846	0.41009924
3297	7	4.751771	1.311368	0.27597458	33.262397	77.6208520	9.1795760	56.0414910	0.42852399	0.16379964
3304	7	4.720004	1.283951	0.27202329	33.040028	66.3024250	8.9876570	18.1672330	0.49832307	0.49471799
3310	6	7.501690	5.525621	0.73658349	45.010140	78.0501680	33.153726	42.1413830	0.57668217	0.78672610
3316	6	8.764610	9.020644	1.02921225	52.587660	97.5978000	54.123864	87.2775900	0.53882014	0.62013472
3320	4	14.32189	42.36729	2.95821920	57.287560	109.875220	169.46916	223.593024	0.52138744	0.75793581
3326	6	6.814245	4.082213	0.59907048	40.885470	98.1730300	24.493278	193.962438	0.41646336	0.12627846
3329	3	1.953990	0.079806	0.04084258	5.8619700	46.7474400	0.2394180	24.7326960	0.12539660	0.00968022
3336	7	13.14614	32.34780	2.46063103	92.022980	97.8849500	226.43460	226.674018	0.94011367	0.99894378
3340	4	13.36264	34.05578	2.54858172	53.450560	145.473540	136.22312	362.657720	0.36742462	0.37562449

Table 8. Summary of total flow units in the reservoirs

Well	XB Reservoir	XC Reservoir	XE Reservoir
A	12	11	10
B	7	0	9
C	8	10	8
Total FU	27	21	27
Overall total flow units = 75			

Conclusion

Depositional environments and subsequent diagenesis are the primary factors controlling porosity distribution, pore connectivity and fluid flow in the three studied reservoirs. The increase in porosity and permeability towards the eastern part of the field reflects lateral change in facies. Well A occurred towards the basin-ward direction in the field and may indicate a shift from mud/silt dominated environment to shoreface/coastal environment where porosity is high. Well C has the best porosity and permeability, lowest water saturation, hence, highest hydrocarbon prospect. The density-neutron crossover is also detected in well C showing the presence of a gas cap.

The stratigraphic Modified Lorenzo Plots (SMLP) revealed a total of seventy five (75) flow units (Table 8) in the three studied reservoirs. Each reservoir displays similar flow pattern relative to others suggesting that facies (rock properties) have a strong control on flow in each reservoir. Generally, poor quality units occur towards the bottom of each reservoir in a well, whereas good quality units occur towards the top. The dominant flow units in the three reservoirs fall within the high storage and flow (normal flow unit) unit category, suggesting that the dominant depositional setting (shallow marine shoreface/beach) and facies type play significant role in fluid dynamic behaviour of sedimentary rock bodies.

Acknowledgement

I appreciate the Department of Petroleum Resources, Port Harcourt, for authorizing the release of this data by the Nigerian Agip Oil Company (NAOC), Port Harcourt. This research was supported financially by Engr. LeBari Nania of Nigeria Agip Oil Company, Port Harcourt, Nigeria. All the authors contributed towards the analysis, interpretation and the writing of this manuscript.

Funding Information

Engineer LeBari Nania of the Nigeria Agip Oil Company, Port Harcourt is appreciated for his financial support during the project research period.

Author's Contributions

Prince Suka Momta: Carried out the MSc research from which the paper was written. He analyzed the data, interprets and wrote the manuscript.

John Owate Etu-Efeotor: Supervised and coordinated the research and read the manuscript.

Charles Ugwu Ugwueze: Reviewed and made some technical inputs in the work.

Ethics

This article is original and contains unpublished material. The corresponding author confirms that all of the other authors have read and approved the manuscript and that there are no ethical issues.

References

Abbaszadeh, M., H. Fujii and F. Fujimoto, 1996. Permeability prediction by hydraulic flow units-theory and applications. SPEFE, 11: 263-271. DOI: 10.2118/30158-PA

Adojoh, O., F. Marret, R. Duller and P. Osterloff, 2014. Relative impact of sea level change and sediment supply on shallow offshore Niger delta margins from palynodebris and lithofacies data. Proceedings of the NAPE Annual International Conference and Exhibitions, Nov. 9-13, Lagos, Nigeria.

Aguilera, R. and M.S. Aguilera, 2002. The integration of capillary pressures and pickett plots for determination of flow units and reservoir containers. SPEREE, 5: 465-471. DOI: 10.2118/81196-PA

Al-Ajmi, F. and S.A. Holditch, 2000. Permeability estimation using hydraulic flow units in a central Arabia reservoir. Proceedings of the Annual Technical Conference and Exhibition, Oct. 1-4, Dallas, TX, pp: 14-14. DOI: 10.2118/63254-MS

Amaefule, J.O., M. Altunbay, D. Tiab, D.G. Kersey and D.K. Keelan, 1993. Enhanced reservoir description: Using core and log data to identify hydraulic (Flow) units and predict permeability in uncored intervals/wells. Proceedings of the 68th Annual Technical Conference and Exhibition of the Society of Petroleum Engineers Held in Houston, Oct. 3-6, Texas, pp: 205-221. DOI: 10.2118/26436-MS

Amajor, L.C. and D.W. Agbaire, 1989. Depositional history of the reservoir sandstones, *Akpor* and Apara oilfields, eastern Niger Delta, Nigeria. J. Petroleum Geol., 12: 453-464. DOI: 10.1111/j.1747-5457.1989.tb00243.x

Archie, G.E., 1950. Introduction to petrophysics of reservoir rocks. Bull. Am. Assoc. Petrol. Geol., 34: 943-961.

Arochukwu, E., 2014. Assessing the impact of reservoir architecture on secondary recovery: A case study of "century" field, Niger delta. NAPE Monthly Technical Meeting, Port Harcourt.

Bhattacharya, S., A.P. Byrnes, W.L. Watney and J.H. Doveton, 2008. Flow unit modeling and fine-scale predicted permeability validation in Atokan sandstones: Norcan East Kansas. Am. Associat. Petroleum Geologists Bull., 92: 709-732. DOI: 10.1306/01140807081

Civan, F., 2003. Leaky-Tube permeability model for identification, characterization and calibration of reservoir flow units. Proceedings of the SPE Annual Technical Conference and Exhibition, Oct. 5-8, Denver, CO, pp: 14-14. DOI: 10.2118/84603-MS

Durogbitan, A.A., 2014. Morphology of the Niger delta: Local facies belts orientation versus depobelts and growth fault orientations. Proceedings of the NAPE Annual International Conference and Exhibitions, Nov. 9-13, Lagos, Nigeria.

Ehrenberg, S.N. and P.H. Nadeau, 2005. Sandstone vs. carbonate petroleum reservoirs: A global perspective on porosity-depth and porosity-permeability relationships. Bull. Am. Assoc. Petrol. Geol., 89: 435-443. DOI: 10.1306/11230404071

Ejedawe, J.E., S.J.L. Coker, D.O. Lambeth-Aikhionabare, K.B. Alofe and E.O. Adoh, 1984. Evolution of oil-generative window and oil and gas occurrence in tertiary Niger delta basin. Am. Associat. Petroleum Geol. Bull., 68: 1744-1751.

Ejedawe, J.E., 1981. Patterns of incidence of oil reserves in Niger Delta Basin. Am. Associat. Petroleum Geol. Bull., 65: 1574-1585.

Evamy, D.D.J., P. Haremboure, W.A. Kamerling, F. Knaap and A. Molloy *et al*., 1978. Hydrocarbon habitat of tertiary Niger delta. Am. Associat. Petroleum Geol. Bull., 62: 1-39.

Gunter, G.W., J.M. Finneran, D.J. Hartmann and J.D. Miller, 1997a. Early determination of reservoir flow units using an integrated petrophysical method. Proceedings of the SPE Annual Technical Conference and Exhibition, Oct. 5-8, San Antonio, TX, pp: 373-381. DOI: 10.2118/38679-MS

Gunter, G.W., J.J. Pinch, J.M. Finneran and W.T. Bryant, 1997b. Overview of an integrated process model to develop petrophysical based reservoir descriptions. Proceedings of the SPE Annual Technical Conference and Exhibition, Oct. 5-8, San Antonio, TX, pp: 475-480. DOI: 10.2118/38748-MS

Knox, G.J. and E.M. Omatsola, 1989. Development of the Cenzoic Niger Delta in terms of the "Escalator Regression" Model and Impact on Hydrocarbon Distribution. In: Proceedings, KNGMG Symposium on Coastal Lowlands, Geology and Geotechonology, W.J.M Van der Linden (Ed.), Dordrecht, Klumer Academic Publishers, pp: 181-202.

Lawal, K.A. and M.O. Onyekonwu, 2005. A robust approach to flow unit zonation. Proceedings of the 29th Annual SPE International Technical Conference and Exhibition, Aug. 1-3, Abuja, Nigeria, DOI: 10.2118/98830-MS

Momta, P.S and M.I. Odigi, 2014. Sequence stratigraphic framework and depositional architecture of MP field, shallow offshore, Niger Delta, Nigeria. Proceedings of the NAPE Annual International Conference and Exhibitions, Nov. 9-13, Lagos, Nigeria.

Perez, H.H., A. Datta-Gupta and S. Mishra, 2005. The role of electrofacies, lithofacies and hydraulic flow units in permeability predictions from well logs: A comparative analysis using classification trees. SPEREE, 8: 143-155. DOI: 10.2118/84301-PA

Porras, J.C., R. Barbato and L. Khazen, 1999. Reservoir flow units: A comparison between three different models in the Santa Barbara and Pirital fields, North Monagas Area, Eastern Venezuela Basin. Proceedings of the SPE Latin American and Caribbean Petroleum Engineering Conference, Apr. 21-23, Caracas, Venezuela, pp: 1-7. DOI: 10.2118/53671-MS

Rahimpour-Bonab, H., A.H. Enayati-Bidgoli, A. Navidtalab and H. Mehrabi, 2014. Appraisal of intra-reservoir barriers in the Permo-Triassic successions of the Central Persian Gulf, Offshore Iran. Geol. Acta, 12: 87-107. DOI: 10.1344/105.000002076

Rahimpour-Bonab, H., H. Mehrabi, A. Navidtalab and E. Izadi-Mazidi, 2012. Flow unit distribution and reservoir modeling in cretaceous carbonates of the Sarvak Formation, Abteymour Oilfield, Dezful embayment, SW Iran. J. Petroleum Geol., 35: 213-236.

Reijers, T.J.A., 2011. Stratigraphy and sedimentology of the Niger Delta. Geologos, 17: 133-162. DOI: 10.2478/v10118-011-0008-3

Rushing, J.A. and K.E. Newsham, 2001b. An integrated workflow model to characterize unconventional gas resources: Part II-Formation evaluation and reservoir modeling. Proceedings of the SPE Annual Technical Conference and Exhibition, Sept. 30-Oct. 3, New Orleans, LA, DOI: 10.2118/71352-MS

Stacher, P., 1995. Present Understanding of the Niger Delta Hydrocarbon Habitat. In: Geology of Deltas, M.N. Oti and G. Postma (Eds.), Taylor and Francis, Rotterdam, ISBN-10: 905410614X, pp: 257-268.

Taslimi, M., E. Kazemzadeh and M.R. Kamali, 2008. Determining rock mass permeability in a carbonate reservoir, southern Iran using hydraulic flow units and intelligent systems. Proceedings of the 2nd IASME/WSEAS International Conference on Geology and Seismology, Feb. 23-25, Cambridge, Uk, pp: 132-139.

Tiab, D. and E.C. Donaldson, 2004. Petrophysics: Theory and Practice of Measuring Reservoir Rock and Fluid Transport Properties. 2nd Edn. Gulf Professional Publishing, ISBN-10: 0080497659, pp: 880.

Weber, K.J. and E. Daukoru, 1975. Petroleum geology of the Niger Delta. Proceedings of the 9th World Petroleum Congress, (WPC' 75), pp: 209-221. DOI: 10.1144/GSL.SP.1990.050.01.21

Yasin, E., C. Patrick and S. Richard, 2001. Hydraulic units approach conditioned by well testing or better permeability modelling in A North Africa oil field. SCA.